Water Resources Research

RESEARCH ARTICLE
10.1029/2025WR040997

Estimating Discharge From Undular Hydraulic Jumps: Feasibility Assessment Based on Flume Experiments

Daniel C. White[1], Elowyn M. Yager[2], Carl J. Legleiter[3], Gordon Grant[4,5], Laura Hempel[6], Christina Leonard[7], Katherine Adler[2], Merritt Harlan[8], and Becky Fasth[5]

[1]Department of Civil and Environmental Engineering, Colorado State University, Fort Collins, CO, USA, [2]Department of Civil and Environmental Engineering, Center for Ecohydraulics Research, University of Idaho, Boise, ID, USA, [3]U.S. Geological Survey, Water Resources Mission Area, Observing Systems Division, Golden, CO, USA, [4]U.S.D.A. Forest Service, Pacific Northwest Research Station, Corvallis, OR, USA, [5]College of Earth, Ocean, and Atmospheric Sciences, Oregon State University, Corvallis, OR, USA, [6]U.S. Geological Survey, Office of Science Quality and Integrity, Pueblo, CO, USA, [7]National Park Service, Water Resources Division, Fort Collins, CO, USA, [8]U.S. Geological Survey, Water Resources Mission Area, Observing Systems Division, Lakewood, CO, USA

Key Points:

- Waves in UHJs exhibit subcritical flow (Fr < 1), with wave celerity matching surface velocity more closely than mean flow velocity
- Adjusting Fr and correcting for $c \neq U$ improves the accuracy of discharge estimates from UHJs
- The refined method enables reliable streamflow estimates from remote sensing without in situ data

Correspondence to:

D. C. White,
danny.white@colostate.edu

Citation:

White, D. C., Yager, E. M., Legleiter, C. J., Grant, G., Hempel, L., Leonard, C., et al. (2026). Estimating discharge from undular hydraulic jumps: Feasibility assessment based on flume experiments. *Water Resources Research*, *62*, e2025WR040997. https://doi.org/10.1029/2025WR040997

Received 8 MAY 2025
Accepted 23 FEB 2026

Abstract Rapids are common in steep rivers, often forming where flow transitions from supercritical (Froude number, $Fr > 1$) to subcritical ($Fr < 1$) through a hydraulic jump. When upstream Fr is supercritical but close to 1, this transition may occur as an undular hydraulic jump, exhibiting a train of stationary waves downstream of the jump toe. Previous studies proposed a method to estimate discharge using only UHJ wave spacing and channel width combined with a wave dispersion equation for large water depths relative to the UHJ wavelength. This method is based on the hypotheses that, by their presence, UHJs indicate near-critical flow conditions ($Fr \approx 1$) and that wave celerity c is equal to and opposite the cross-sectionally averaged flow velocity U. However, these hypotheses have not been thoroughly tested. We used data from published UHJ flume experiments to test the hypotheses that $Fr \approx 1$ and $c = U$, compare the deep-water and general wave dispersion equations, and evaluate the accuracy of discharge estimates. In these experiments, the stationary waves exhibited shallow depths relative to wavelength and flow was subcritical ($Fr < 1$) when averaged across multiple wavelengths. Additionally, wave celerity more closely approximated the surface flow velocity than U. By using a Fr representative of actual conditions and applying a coefficient to correct for $c \neq U$, the accuracy of the discharge estimates improved. This finding suggests that the critical flow-based method is robust and can produce reliable streamflow estimates if the remotely observed wave trains are correctly interpreted as UHJs, without requiring in situ measurements.

1. Introduction

Non-contact discharge measurement techniques obviate the need to stand or place an instrument in a river. Such methods can be used to measure flow in steep rivers that can be difficult to access and potentially dangerous. Inferring discharge from remotely sensed data can be approached in a variety of ways, such as through calibration with in situ data or roughness-based methods (e.g., Bjerklie et al., 2005; Durand et al., 2023) but often involves calculating the product of channel width, depth, and velocity. Width can be measured easily from an image of a river, surface flow velocities can be derived from image time series (Jodeau et al., 2008; Le Coz et al., 2014; Legleiter & Kinzel III, 2021; Schweitzer & Cowen, 2021), and depths can be estimated via spectrally based methods (Kasvi et al., 2019; Legleiter, 2021; Legleiter et al., 2009). However, established methods for estimating velocity are often contingent upon the presence of trackable features such as floating material or high turbidity whereas estimating depth typically requires clear water.

An alternative approach is based upon features of the water surface itself. Legleiter et al. (2025), building on work by Dietterich et al. (2022), proposed a new technique to estimate river discharge that involves measuring the wavelength of stationary waves identified in remotely sensed river imagery. These stationary waves, hereafter referred to as standing waves, are periodic surface undulations that remain fixed in space and time while the water itself flows through them. Proceeding downstream from where the surface oscillations begin (the jump toe), UHJs represent a transition from super-to subcritical flow over a distance of multiple waves rather than a single hydraulic jump or roller.

Several analytical and numerical models have been developed to estimate the free-surface profile and velocity distribution through UHJs (e.g., Castro-Orgaz & Chanson, 2022; Castro-Orgaz et al., 2015; Grillhofer &

Schneider, 2003; Jurisits & Schneider, 2012; Montes & Chanson, 1998; Roy Biswas et al., 2021). These frameworks employed in these models range from weakly non-linear wave theory and Boussinesq-type equations to fully non-hydrostatic, Reynolds-averaged Navier–Stokes (RANS) and large-eddy simulations (LES). Numerical models can reproduce measured free-surface and velocity profiles with high fidelity and have clarified how dispersion, non-hydrostatic pressure, and turbulence interact in UHJs. A review by Castro-Orgaz and Chanson (2022) synthesizes these developments, showing how progressively more sophisticated formulations capture wave formation, decay, and three-dimensional flow structures.

Although substantial progress has been made through these theoretical and/or numerical studies, the emergence of new approaches to remotely estimate discharge of high energy flows from measured wavelengths of standing waves motivates a closer examination of the underlying assumptions and principles governing the architecture of UHJs. In particular, we seek to use data from published flume experiments to test the validity of fundamental assumptions used in these novel methods. Furthermore, no studies have investigated the relationship between theoretical wave celerity and depth-averaged velocity in UHJs. Establishing such relationships could enhance non-contact discharge estimation methods, particularly in high-energy or inaccessible settings where traditional gauging of a stream is impractical.

Dietterich et al. (2022) and Legleiter et al. (2025) take a wave-centric approach, assuming that flow within the standing waves themselves is near-critical and applying wave dispersion relationships to infer both velocity and depth from measurements of wavelength and width made from readily available image data. This bypasses the need for measurements of upstream Froude and depth but could also introduce uncertainty if the Froude number across standing waves is not equal to 1. Herein, we explicitly evaluate these assumptions and examine UHJ flow conditions to assess the feasibility of inferring discharge from remotely sensed data.

The behavior of UHJs has often been discussed alongside the broader theory of standing waves because both involve free-surface undulations that can appear stationary relative to the channel. Kennedy (1961) showed that standing wave trains result when the downstream flow velocity is equal and opposite to the wave celerity c, also known as phase speed. These standing waves can be observed in mobile bed channels where dunes or antidunes occur (Kennedy, 1963; Recking et al., 2009) and in fixed-bed channels (Castro-Orgaz et al., 2017; Chanson & Montes, 1995; Grillhofer & Schneider, 2003). Kennedy suggested that the condition in which waves do not propagate up- or downstream indicates that specific energy is minimized (i.e., critical flow, $Fr = 1$). The Froude number, Fr, is the ratio of inertial to gravitational forces and is defined as $Fr = U/\sqrt{gD}$, where U is the cross-sectionally averaged flow velocity, g is acceleration due to gravity, and D is the hydraulic depth ($D = A/T$, with A the cross-sectional area and T the top width). Although UHJs involve non-hydrostatic pressure fields and vertical accelerations (e.g., Castro-Orgaz et al., 2015), we adopt the classical specific energy definition for consistency with previous UHJ and remote-sensing-based approaches, noting that the specific energy relation provides a useful approximation in this context. Specific energy for a given discharge and channel geometry is defined as $Q^2/2gA^2 + h$ where Q is discharge and h is water depth measured from the channel bed. In the case of a rectangular channel, D reduces to h and $A = hB$ (with B the channel width), giving Equation 1 in the form used throughout this paper.

$$Fr = \frac{U}{\sqrt{gh}} \tag{1}$$

In deep water, the wave celerity is given by

$$c_d = \sqrt{\frac{gL}{2\pi}} \tag{2}$$

where L is wavelength (Lamb, 1924; Pond, 1983). By conservation of mass, discharge, Q, can be computed as $Q = \mathrm{UA}$, or $Q = UhB$ where the channel is assumed to be rectangular. Dietterich et al. (2022) showed that by assuming that $Fr = 1$ and $c_d = U$, Equations 1 and 2 can be solved for velocity as $U = \sqrt{\frac{gL}{2\pi}}$ and then depth as $h = L/2\pi$. Q can thus be calculated from measurements of wavelength and width as

$$Q_d = B\sqrt{g\left(\frac{L}{2\pi}\right)^3} \quad (3)$$

where the subscript d indicates that the discharge estimate is based on the deep-water wave dispersion relation (Equation 2).

This approach involves three primary assumptions regarding the relationships among discharge, wavelength, cross-sectionally averaged velocity, and the celerity of standing waves:

1. Near-critical flow averaged through an UHJ ($Fr \approx 1$),
2. Deep-water conditions ($h/L > 0.5$), and
3. Wave celerity and cross-sectionally averaged flow velocity are equal ($c = U$).

We note that assuming $Fr = 1$ and $c = U$ implies that wave celerity equals $\sqrt{gh}$, the shallow-water gravity wave speed. This equivalence provides additional motivation to examine assumption 3.

Legleiter et al. (2025) found that by applying these assumptions, the method to estimate discharge worked well, however, the validity of the assumptions has not been examined systematically in controlled laboratory experiments. Because their framework relies on the interpretation of remotely observed wave trains as UHJs, its broader applicability depends on that classification. There are many studies describing standing waves through UHJs in fixed-bed, rectangular flumes. The idealized conditions captured in these experiments provide an opportunity to conduct a more detailed evaluation of the feasibility of inferring discharge from hydraulically verified UHJs.

The conditions necessary for UHJ formation have been studied extensively and UHJs have been shown to form at an inlet Froude number (Fr_1) ranging from 1 to approximately 1.7 (Chanson, 2009; Chanson & Montes, 1995; Chow, 1959; Montes & Chanson, 1998). However, further research is needed to test the three specific assumptions listed above for discharge estimation. Castro-Orgaz et al. (2017) and Chanson (2009) have shown that flow depth is near critical in troughs downstream of the first wave in UHJs, which Dietterich et al. (2022) also demonstrated. Although the average Froude number across an undular hydraulic jump can be derived theoretically from momentum principles (e.g., Belanger equation; Chanson, 2004; Chow, 1959; Henderson, 1966; Sturm, 2001), we are not aware of any experimental studies that have directly measured and evaluated the Froude number along a sequence of standing waves using a larger sample size or that related wave celerity to U.

In this study, we investigate assumptions 1–3 by revisiting experimental flume data collected across five experiments (Chanson & Montes, 1995; Hu et al., 2023; Montes & Chanson, 1998; Ohtsu et al., 2003; Pasha & Tanaka, 2017; Reinauer & Hager, 1995). Moreover, we test the discharge estimation method outlined by Legleiter et al. (2025), and summarized in Equation 3, by calculating discharges for the various flume data sets based on these assumptions. We also propose a new method that links a more general wave dispersion equation to the definition of the Froude number to enable discharge estimation in the more general case where the deep-water condition is not satisfied.

2. Methods

2.1. Flume Data

The data used in our analysis were collected in studies conducted at the Hydraulic Laboratory at the University of Queensland (Chanson & Montes, 1995; Montes & Chanson, 1998), the VAW Laboratory at ETH Zürich (Reinauer & Hager, 1995), Nihon University (Gotoh et al., 2004; Ohtsu et al., 2001, 2003), Saitama University (Pasha & Tanaka, 2017, 2019), and the State Key Laboratory of Hydraulics and Mountain River Engineering (Hu et al., 2023). We refer to these experimental data sets using acronyms of the authors' surnames such that Ohtsu et al. (2001) is OYG, Chanson and Montes (1995) is CM, Pasha and Tanaka (2017) is PT, Reinauer and Hager (1995) is and Hu et al. (2023) is HWPWB (Table 1). In each of these studies, common characteristics observed for UHJs include upstream supercritical flow and multiple standing waves with well-defined peaks and troughs.

Table 1
Overview of Flume Data Analyzed in This Study

Data set	Referenced manuscripts	Q (m^3/s)	Fr_1	Re_1 ($\times 10^4$)	B (m)	S (%)	L (m)
CM	(Chanson, 1993; Chanson & Montes, 1995; Montes & Chanson, 1998)	0.0049–0.0301	1.05–2.71	2.0–12.0	0.25	0.3–2.1	0.21–0.75
OYG	(Gotoh et al., 2004; Ohtsu et al., 2001, 2003)	0.0022–0.1228	1.14–2.99	1.3–16.4	0.105–1.65	0.0	0.19–0.88
PT	(Pasha & Tanaka, 2017, 2019)	0.0079–0.0289	0.70–1.96	1.1–4.1	0.7	0.2	0.09–0.40
RH	Reinauer and Hager (1995)	0.0084–0.0818	1.2–1.89	1.7–16.4	0.5	0	0.225–1.8
HWPWB	Hu et al. (2023)	0.104	1.89	8.4	1.4	0	0.52

Note. Q is discharge, Fr_1 is inflow Froude number, Re_1 is inflow Reynolds number, B is channel width, S is channel slope, and L is undular hydraulic jump wavelength.

We use measurements that are consistent across all studies, including width, B, the distance between first and second wave peaks, L, flow depth at the first peak, h_p, and flow depth at the first trough, h_t; the only analyzed data were measurements at the channel centerline. We assume cross-sectionally uniform flow depth and use the reported depth and discharge to estimate the cross-sectionally averaged velocity U as discharge divided by cross-sectional area Q/A and calculate the measured Fr at the first peak, Fr_p, and first trough, Fr_t, using Equation 1. We take the average of the measured Fr_t and Fr_p which we term Fr_{ave}. Although not explicitly described for some flume runs, the UHJs observed in these studies did not necessarily occupy the entire channel width and lateral shockwaves could undermine, to some degree, the assumptions of cross-sectionally uniform flow depth and wavelength. Assuming cross-sectionally uniform flow and the use of the channel centerline depth h to determine measured Fr could produce errors. Because flow near the walls is slower, the measured Fr may be an overestimate of cross-sectionally averaged conditions.

The channel widths in these experiments ranged from 0.105 to 1.65 m, and channel slopes tested include 0% (Gotoh et al., 2004; Hu et al., 2023; Ohtsu et al., 2001, 2003), 0.33%–2.48% (Chanson, 1993; Chanson & Montes, 1995), and 0.2% (Pasha & Tanaka, 2017) The channel walls and bed used in all experiments were either glass or steel. Inlet Froude number, Fr_1, ranged from 0.7 to 2.99, and wavelength, L, ranged from 0.09 to 1.8 m. Although these flume experiments described UHJ wave characteristics in relation to inflow Froude number, Fr_1, none explicitly evaluated whether $c = U$ in UHJs using theoretically derived equations (i.e., Equation 2) or whether the assumption of the UHJ averaged Fr (Fr_{ave}) = 1 is appropriate. For each experiment, we also estimated an inflow Reynolds number Re_1 to provide a general indication of flow regime. When inflow depth and discharge were reported, we computed $\text{Re}_1 = U_1 h_1/\nu$ with $\nu = 1.0 \times 10^{-6}$ m^2 s^{-1}. When inflow depth was not explicitly reported but Fr_1, Q, and B were available, we estimated h_1 from Fr_1 and then computed Re_1. Reported Reynolds numbers range from 10^4–10^5, implying that flows within these laboratory flumes were fully turbulent. A summary of the flume data used in this analysis is presented in Table 1.

To first investigate the assumption that flow is near critical in UHJs (assumption 1), we visually examined the longitudinal variation of Fr for the PT data set, which included continuous centerline depth measurements along the entire length of the flume across multiple jump wavelengths. The PT study was the only one that included full longitudinal profiles of depth from many examined experiments, whereas CM, OYG, and RH present depth measurements at peaks and troughs. Additionally, we analyze the distribution of Fr_p, Fr_t, and Fr_{ave} across 319 experiments from the PT, OYG, CM, and RH data sets and perform a single-sample t-test of the null hypothesis that the means of Fr_p, Fr_t, and Fr_{ave} are all equal to 1 to further directly test assumption 1. We directly test assumption 2 by computing h_{ave}/L, where h_{ave} is the average of h_p and h_t, to determine the depth condition for all flume runs. The results of this analysis led us to investigate methods to account for the influence of shallow depths on wave celerity (Section 2.2) and the assumption of $c = U$ (assumption 3), as described further in Section 2.4.

2.2. New Method of Discharge Calculation for Shallow Depths

According to linear wave theory, the celerity of a gravity wave depends on wavelength for any flow depth, but this dependence is weaker in shallower water (Airy, 1845; Phillips, 1977; Stokes, 1847). The criterion used to distinguish between deep and shallow water is the ratio of water depthto wavelength; if $h/L > 0.5$, the water is considered deep. In deep water, wave celerity, c_d, is related to wavelength via Equation 2. However, the general form of the wave dispersion equation for linear gravity waves that applies to all depths is given by

$$L = \frac{2\pi {c_g}^2}{g} \coth\left(\frac{2\pi h}{L}\right) \tag{4}$$

where coth denotes the hyperbolic cotangent and c_g is celerity. In this study, we refer to Equation 4 as the general wave dispersion relation. This expression can be rearranged to solve for celerity:

$$c_g = \sqrt{\frac{gL}{2\pi} \tanh\left(\frac{2\pi h}{L}\right)}. \tag{5}$$

The primary difference between the deep-water (Equation 2) and general (Equation 5) wave dispersion relations is that Equation 5 includes a depth-dependent term from linear wave dispersion theory, which represents the effect of finite depth on wave celerity.

UHJs are not necessarily restricted to deep water where $h/L > 0.5$, and a more general approach to estimating discharge would involve the general dispersion relation (Equation 5) instead of Equation 2. By assuming $c_g = U$, Equations 1 and 5 were solved simultaneously for depth by minimizing the following objective function

$$0 = Fr\sqrt{gh} - \sqrt{\frac{gL}{2\pi} \tanh\left(\frac{2\pi h}{L}\right)}. \tag{6}$$

To solve for h, we selected a specific value of Fr and used an optimization algorithm to minimize the sum of squares of Equation 6. Once we had h, U was then calculated using the Froude number equation (Equation 1). Discharge can thus be computed for any depth using $Q_g = UhB$, where the subscript g refers to the general wave dispersion equation. We evaluate discharge by applying both the deep-water and general dispersion relations; by comparing performance across these formulations, we assess whether the $c = U$ approximation used in Equation 3 is sufficient and whether explicitly solving the full dispersion relation might provide improved estimates.

The difference between the deep-water and general wave dispersion equations is highlighted by setting Equation 2 and Equation 5 equal to $Fr/\sqrt{gh}$, and solving for h over a range of Fr and L. For $Fr < 1$, as Fr approaches 1, estimated flow depth remains greater than 0 using the deep-water dispersion equation (Figure 1a) whereas estimated depth approaches 0 using the general dispersion relation (Figure 1b). This difference arises as a result of the tanh term in Equation 5, which accounts for the influence of flow depth on wave celerity. Similarly, h/L diverges when comparing Equations 2 and 5 across a range of $c/\sqrt{gh}$, which is equivalent to Fr when $c = U$ and $Fr = c/\sqrt{gh}$. The ratio h/L approaches 0 using Equation 5 when $c/\sqrt{gh}$, and thus Fr, by assumption 1, approaches 1 (black dashed line in Figure 1c).

Given these differences between the two wave dispersion equations, we used both to estimate discharge, assess their relative accuracy, and evaluate whether assuming deep water (assumption 2) produces reasonable predictions. We estimated discharge using measurements of h and L taken in the 319 experimental flume runs and compared these calculated discharge values with those reported for each experiment. The HWPWB data set was not included in these analyses because it consisted of only one experiment. We tested whether assumption 1 ($Fr \approx 1$) is needed for accurate discharge predictions by estimating discharge using both equations with a range of input assumed Fr from 0.5 to 1.1. For the deep-water dispersion equation, this analysis involved rearranging Equations 1 and 2 to solve for Q_d including the Fr term, such that

$$Q_d = \frac{B}{Fr^2}\sqrt{g\left(\frac{L}{2\pi}\right)^3}. \tag{7}$$

Equation 7 differs from Equation 3 because Fr is assumed to be 1 in Equation 3 and thus does not appear in the expression. However, we include Fr here to investigate the potential to improve discharge estimates by allowing for the possibility of a Fr value other than 1. We quantify the accuracy of the discharge estimation methods using the same metric as Durand et al. (2016) in their comparison of five algorithms for remote sensing of discharge in natural rivers, the relative root mean squared error (RRMSE):

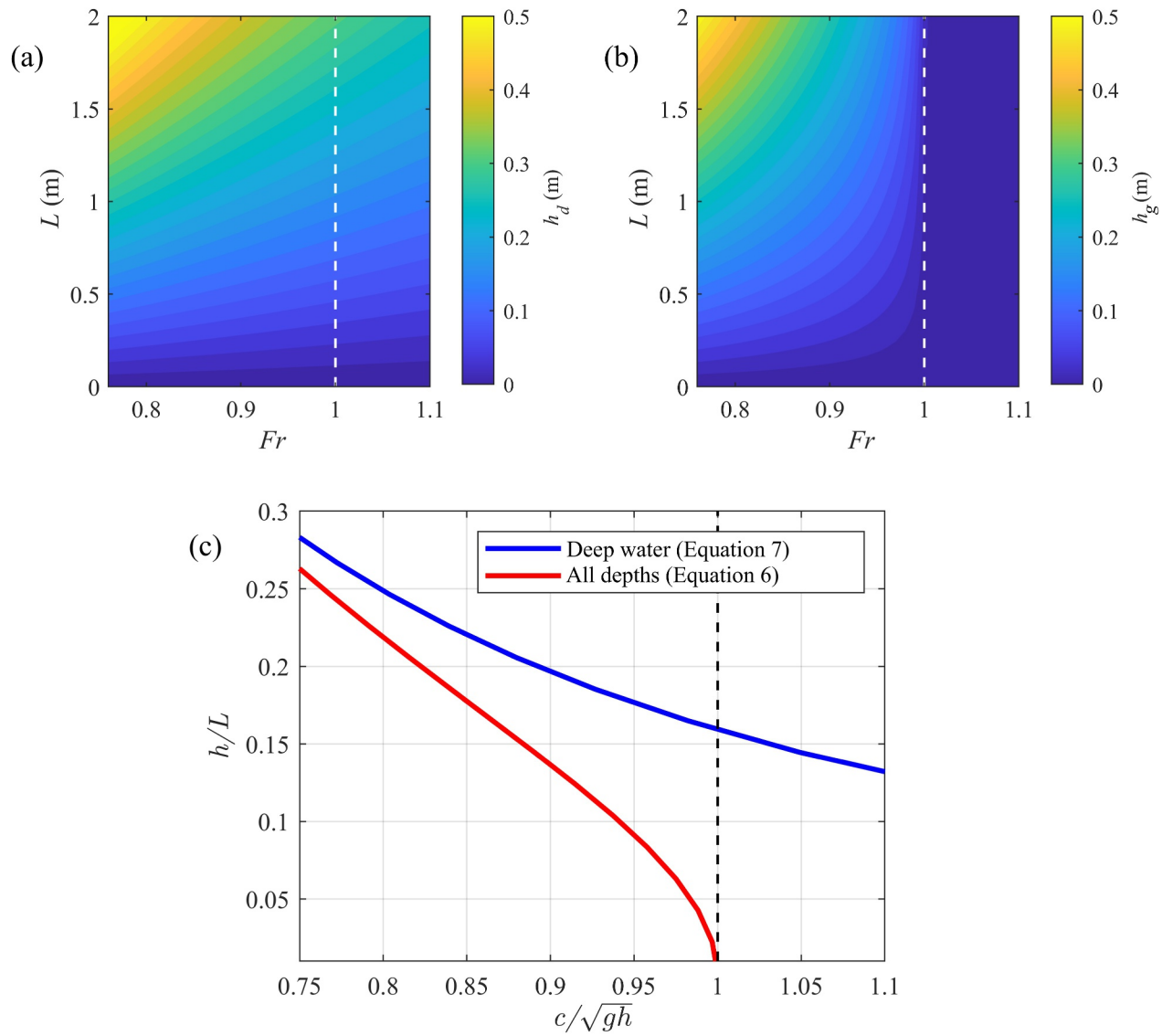

Figure 1. Contour map of computed flow depth values as functions of the assumed Froude numbers and wavelengths using the (a) deep-water wave dispersion equation, and (b) the general dispersion equation. Panel (c) $c/\sqrt{gh}$ versus h/L for the deep and general wave dispersion equations.

$$\text{RRMSE} = \sqrt{\frac{\frac{1}{n}\sum_{j=1}^{n}(Q_j - Q_{kj})^2}{\sum_{j=1}^{n} Q_{kj}^{\,2}}} \tag{8}$$

where n is the number of observations, Q_j is the jth estimated discharge, and Q_{kj} is the jth known discharge. We identify the assumed Fr that minimizes RRMSE to assess whether $Fr = 1$ must be assumed to calculate discharge. We perform a linear regression analysis of the estimated versus known discharge values using both the deep-water and general dispersion equations and use the coefficient of determination (R^2) as a summary metric of agreement. We note that a high R^2 in this application does not necessarily suggest accuracy, but low variance in the known vs. estimated discharge estimates.

2.3. Sensitivity Analysis

We used a differential approach to analyze the sensitivity of discharge to assumed Fr to assess the potential to improve the accuracy of discharge estimates by selecting a Fr i.e. more representative of measured conditions. In general, this type of analysis involves calculating the incremental change of a function $f(x)$ with respect to the change of an independent variable, x

$$\Delta f(x) = f'(x)\Delta x. \tag{9}$$

where $\Delta f(x)$ is the incremental change of a function of x and $f'(x)$ is the derivative of $f(x)$ with respect to x. In this case, we take derivatives of the equations for estimating discharge using the deep-water and general wave dispersion equations. For deep-water, we use the form of Equation 3 that includes Fr such that

$$q_d = \frac{1}{Fr^2}\sqrt{g\left(\frac{L}{2\pi}\right)^3} \tag{10}$$

where q_d is the discharge per unit width (Q_d/B) and take its derivative with respect to the independent variable Fr

$$\frac{\partial q_d}{\partial Fr} = -\frac{2}{Fr^3}\sqrt{g\left(\frac{L}{2\pi}\right)^3} \tag{11}$$

where we vary Fr from 0.5 to 1.1.

The general wave dispersion equation does not have an analytical solution, so we used a numerical approximation of the derivative of q_g, the unit discharge with respect to Fr using the general dispersion relation

$$\frac{\partial q_g}{\partial Fr} \approx \frac{\Delta q_g}{\Delta Fr} \tag{12}$$

where Δq_g represents a difference in estimated discharge values over incremental steps of Fr (ΔFr), where Fr is varied from 0.5 to 1.1 in steps of 0.01. For the sensitivity analysis of discharge estimation to variation in Fr, we fixed L at 0.45 m, the median value of the experimental data.

2.4. Wave Celerity vs. Flow Velocity

To investigate assumption 3, we compare measured velocity and estimated celerity using both Equations 2 and 5 for the PT, OYG, RH, and CH data sets. We use the average velocity of the first peak and trough which we term U_{ave}. We computed c_d using measurements of L, and c_g using measurements of h and L in each experiment. In comparing c_d and c_g with U_{ave}, we acknowledge that differences between the two could be due to four factors, namely: (a) c estimated by Equations 2 and 5 could be incorrect because of error inherent to the equations themselves, (b) c estimates could have uncertainties because of the measurements of h_{ave} and L used in its estimation, (c) uncertainty in U_{ave} because it is calculated using centerline depth instead of average channel depth across the width of the flume, and (d) that the measured cross-sectionally averaged velocity does not represent celerity.

To reduce uncertainty when comparing estimates of c and U_{ave}, we also analyzed detailed velocity measurements in an UHJ from the HWPWB data set. We used their measurements of downstream velocity spaced at 1-mm vertical increments throughout the water column, made at three locations across the channel at the first three wave peaks and troughs of an UHJ. From these data, we computed the cross-sectionally averaged velocity and the width-averaged surface velocity at each peak and trough, then compared them with computed wave celerity using the deep-water and general wave dispersion equations.

We defined a proportionality constant, α, as the ratio of cross-sectionally averaged velocity to surface velocity. This ratio has its foundation in the theory of open-channel flow, where models based on the logarithmic velocity profile describe the link between mean and surface velocity (e.g., Chow, 1959; Keulegan, 1938). However, we emphasize that UHJ conditions deviate from uniform flow due to non-hydrostatic pressure gradients, local accelerations, and turbulence. In general, the relationship between depth-averaged and surface velocity could be tested using high-fidelity numerical solutions that resolve the flow field in UHJs (e.g., Roy Biswas et al., 2021). In

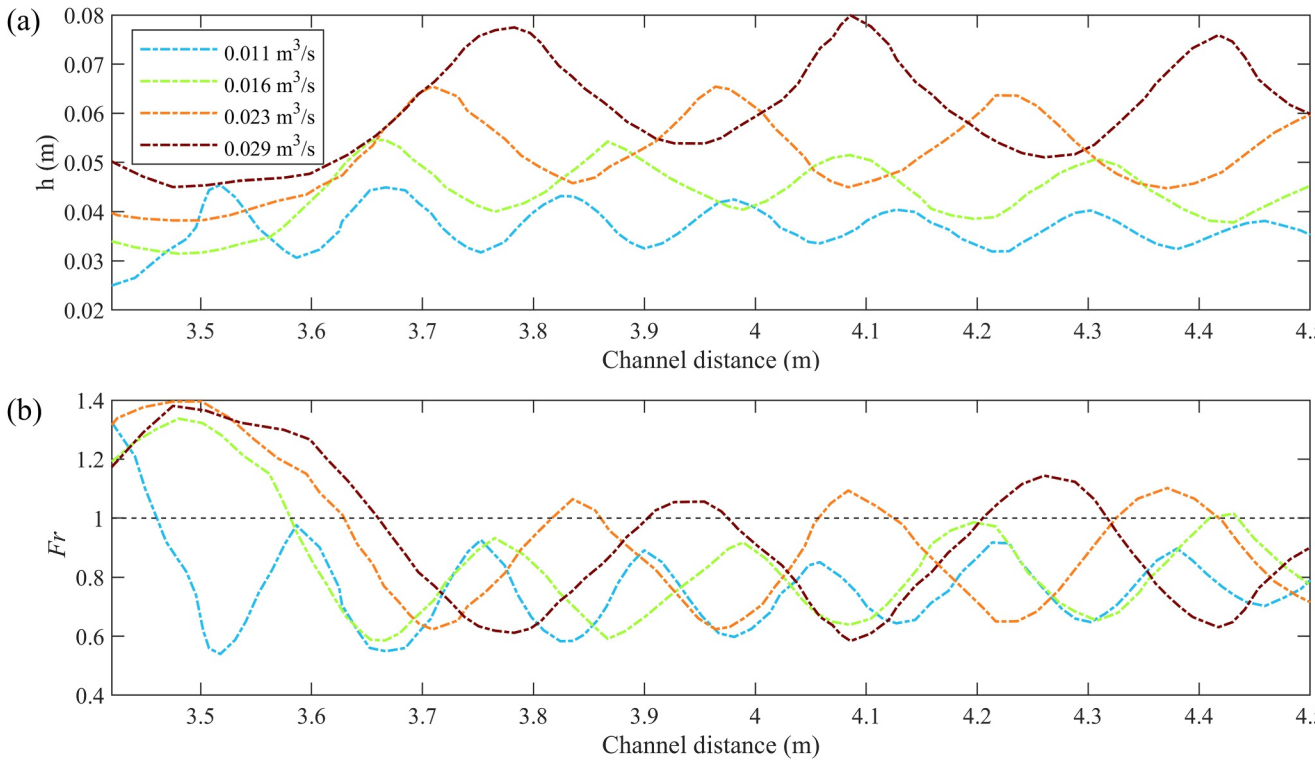

Figure 2. UHJ flow conditions for a subset of experimental runs by PT labeled by discharge (a) Channel centerline flow depth through multiple standing waves. Panel (b) Fr through multiple standing waves. Black dashed line represents critical flow, $Fr = 1$.

this study, however, we use α solely as an empirical scaling factor and compare it with values reported for natural rivers (Biggs et al., 2023) because our overarching goal is to apply this method to estimate flow velocity and discharge in natural rivers using remotely sensed imagery. This pragmatic approach to defining α thus satisfies our immediate objectives, but we also recognize the opportunity to integrate UHJ-specific models and velocity-celerity relationships. For this analysis, we applied α to estimate discharge using the deep-water and general wave dispersion equations. In our investigation of assumption 3 ($c = U$) we avoid conflating possible error associated with the assumption 1, that $Fr = 1$, and instead we use the measured Fr_{ave} for each experiment.

Lastly, we explore opportunities to improve the accuracy of this method by relaxing assumptions 1–3 to account for conditions when $Fr \neq 1$, deep-water conditions are not met, and $c \neq U$ by developing an approach to discharge calculation using a wave dispersion equation that applies to all depth conditions and accounts for the sensitivity of both the deep-water and general wave dispersion equations to variation in Fr.

3. Results

3.1. Measured *Fr*

To investigate the hypothesis that flow is near critical in UHJs (assumption 1), we examine the centerline profiles of depth and Fr for a subset of the PT data set (Figure 2). Flow is supercritical at the upstream end of the experimental section such that $Fr_1 > 1$ and energy is then dissipated through a series of standing waves where Fr fluctuates around a subcritical value, approaching critical in the troughs in some flume runs (Figure 2b). When analyzing water surface and Fr profiles from all PT flume runs, a small subset of which is shown in Figure 2, a general pattern emerges: Fr approaches but rarely exceeds 1 in the troughs.

To further investigate the hypothesis that $Fr = 1$ in UHJs, we expand the analysis to all flume studies described in Section 2.1 and assess the distribution of measured Fr calculated using the measured discharge and centerline depth measurements taken at the first wave trough and peak for all runs (Figure 3). The mean Fr is 0.94 at troughs and 0.54 at peaks. A single sample t-test leads to rejection of the null hypothesis that the mean Froude at the peak, Fr_p, is equal to 1 at a 5% significance level. Similarly, the null hypothesis that the mean Froude at the trough, Fr_t,

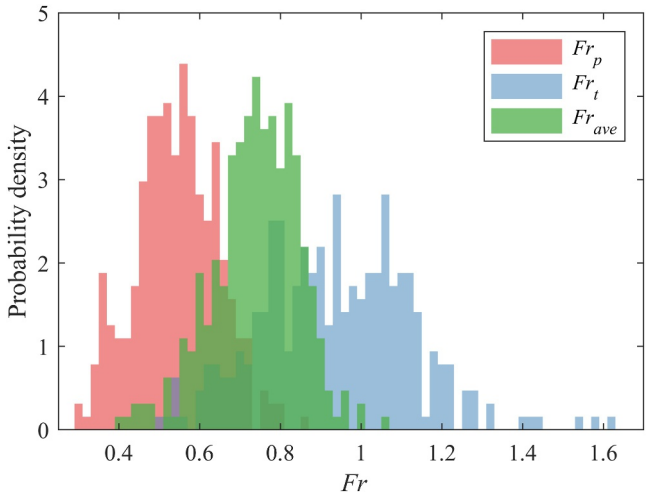

Figure 3. Histogram of computed Froude values at the first trough (blue bars), the first peak (red bars), and the average of both (green bars). The total number of data points included in the distribution is 319.

is equal to 1, is also rejected at a 5% significance level. Additionally, the distribution of Fr_{ave} has a mean of 0.74, which also differs from 1 at a 5% significance level. Only 39% of Fr_t values exceeded 1 and none of the Fr_p values exceed 1. These results indicate that in most cases, Fr approaches but rarely surpasses 1 through the troughs of UHJs and never exceeds 1 at wave crests. Moreover, Fr averaged over the length of the UHJs does not generally equal 1 as stated in assumption 1.

3.2. Depth Condition

We computed the measured h_{ave}/L, where h_{ave} is the average of the measured h_p and h_t, to determine the depth condition for all flume runs. We found that the mean h_{ave}/L was 0.2, much lower than the criterion for deep water ($h/L > 0.5$). Values for h_{ave}/L ranged from 0.07 to 0.37 across all flume runs, thereby implying assumption 2 was not strictly correct for these experiments. These findings are consistent with prior work showing that simplified wave models lose predictive skill in energetic UHJ conditions. For example, Chanson and Montes (1995) found that measured wavelengths closely follow Boussinesq predictions at low Froude numbers but deviate at higher values as specific energy increases. Here, we also observe that deep-water wave assumptions are not satisfied across many UHJ conditions, which further underscores the need to evaluate wave-based discharge methods against the full dispersion relation rather than relying on deep-water approximations. We therefore tested the deep-water wave dispersion relation (Equation 2) with $Fr = 1$ to assess how all assumptions affect discharge estimate results. We then test both the deep and general dispersion relations for a range of Fr to determine how depth condition and Fr affect discharge estimate results and compare estimated discharge values with the reported values for all the flume experiments.

3.2.1. Discharge Estimate

We combined the deep-water wave dispersion equation (Equation 3) and the definition of the Froude number to estimate discharge (Q_d) as a function of measured L and B with $Fr = 1$. These estimated Q_d generally matched the measured Q values (Figure 4). A linear regression of the estimated compared to known values gave a slope coefficient of 0.94 and an R^2 value of 0.77. The RRMSE of the Q_d estimates was 0.35, which is comparable to remote discharge error estimates in natural rivers described by Durand et al. (2016). Despite assumptions 1 ($Fr \approx 1$) and 2 ($h/L > 0.5$) not being met, the estimated discharges exhibit scatter but remain distributed about the 1:1 line ($R^2 = 0.77$; RRMSE $= 0.35$), relative to measured values. This motivated an assessment of the sensitivity of Q_g and Q_d to a wider range of expected Fr and assessment of assumption 3 ($c = U$).

3.3. Sensitivity Analysis

We estimated both Q_d and Q_g for a range of assumed Fr ($0.75 < Fr < 1.1$) for each experiment. We compared the RRMSE for these flume data at each assumed Fr and found that RRMSE was minimized at $Fr = 0.87$ for the general dispersion relation (Figure 5, orange curve) and at $Fr = 1.05$ for the deep-water relation (Figure 5, blue curve). At $Fr \geq 1$ the general dispersion relation resulted in a RRMSE of 1 because estimated discharge was approximately 0. This occurred because predicted depth approaches 0 as Fr approaches 1 (refer to Figure 1b).

We also explored the sensitivity of unit discharge estimates to variation in Fr using a differential approach but did not use measured flume data for this analysis. Rather, we specified L, computed q_g, and q_d, and calculated how incremental changes in Fr influenced estimated discharge. This analysis served to quantify the potential error associated with the choice of Fr. We showed resulting q_d (Figure 6a) and q_g (Figure 6c) at $L = 0.45$ for $0.75 < Fr < 1$. As Fr approached 1, the slope of the $\partial q_d/\partial Fr$ curve leveled off and the magnitude of $\partial q_d/\partial Fr$ approached 0, suggesting that at near-critical Fr values, q_d is less sensitive to variation in Fr. For the general wave dispersion relation, q_g was least sensitive at $Fr = 0.85$, and then increased in sensitivity again as Fr approached 1 (refer to Figure 6d). This theoretical differential sensitivity analysis produced patterns which can be compared with the RRMSE curves for the flume data (Figure 5). At Fr values where the absolute value of the magnitude of $\partial q/\partial Fr$ value was lowest, Q_d and Q_g estimates had the lowest RRMSE (i.e., the discharge estimates were the most

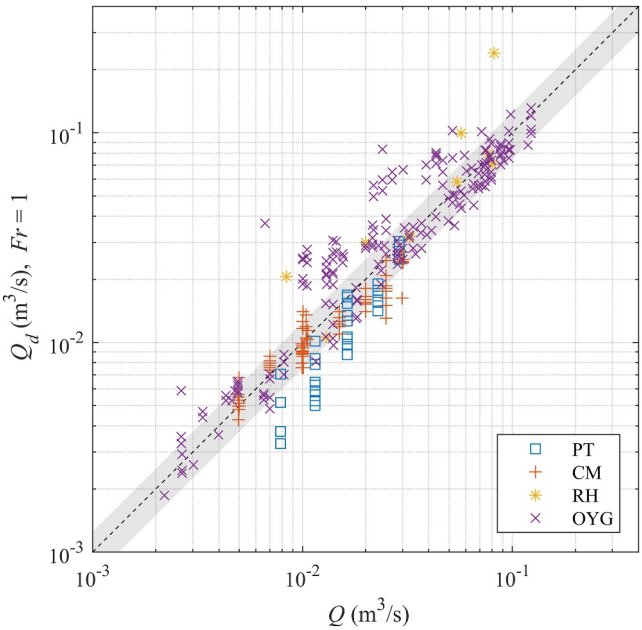

Figure 4. Estimated (y-axis) versus known (x-axis) discharge for four UHJ experimental data sets using $Fr = 1$. The gray band represents 25% error range and the black dashed line is the 1:1 line.

accurate). For example, when using the general dispersion equation and selecting $Fr = 0.85$, or the value at which the slope of the Fr versus $\partial q_g/\partial Fr$ curve was 0, the RRMSE was 0.35, comparable to other methods for remote sensing of river discharge (Andreadis et al., 2025; Durand et al., 2016).

Although we reported the sensitivity of changes in discharge to changes in Fr for a selected $L = 0.45$ m, the slope of the Fr versus $\partial q_g/\partial Fr$ curve was minimized at $Fr = 0.85$, and the slope of the Fr versus $\partial q_d/\partial Fr$ curve was low at and above $Fr = 1$ independent of L. In other words, for all L values, the curves presented in Figures 6b and 6d would exhibit the same location at which the slope is zero (approaching $Fr = 1$ for $\partial q_d/\partial Fr$, and at $Fr = 0.85$ for $\partial q_g/\partial Fr$).

3.4. Discharge Error Using Known *Fr*

Rather than assuming a fixed Fr for all Q_d and Q_g estimates (i.e., $Fr = 1$), we also estimated discharge using Fr_{ave}, the average Fr over the first peak and trough for each experiment. In doing so, we isolated potential sources of error related to the assumptions that $c = U$ and that the flow was deep relative to the wavelength. We found that both Q_d and Q_g generally overpredicted Q using Fr_{ave} (Figure 7), and that Q_d had less scatter but more points falling outside the gray 25% error bounds (Figure 7a). The Q_g estimate was more accurate, with an RRMSE of 0.53, compared to 0.77 for Q_d. The linear trendline of Q versus Q_d had a slope coefficient of 1.48 and an R^2 of 0.86. For Q versus Q_g, the slope coefficient was 1.2 with an R^2 of 0.82. Using Fr_{ave} led to a decrease in performance using the deep-water equation compared with an assumption that $Fr = 1$. However, the scatter of points of estimated versus known discharge in Figures 7a and 7b, was quite similar to Figure 4, though overprediction occurred. This may indicate that when Fr is known, there could be other factors that contribute to the error such as the assumption that $c = U$.

The tendency for both Q_d and Q_g to overpredict discharge when using measured Fr_{ave} could be a consequence of the complex flow structure in UHJs. Local Froude numbers at peaks and troughs are influenced by free-surface curvature, vertical accelerations, and departures from hydrostatic pressure conditions, which can alter pointwise Fr relative to a purely depth-averaged momentum balance. In this context, using these local values as a proxy for a cross-sectionally averaged condition could bias depth and celerity estimates and lead to systematic overprediction of discharge. These patterns are consistent with UHJs exhibiting some degree of nonhydrostatic and three-dimensional behavior, although additional detailed measurements of velocity and pressure distributed across the full width of the channel would be needed to fully quantify these effects.

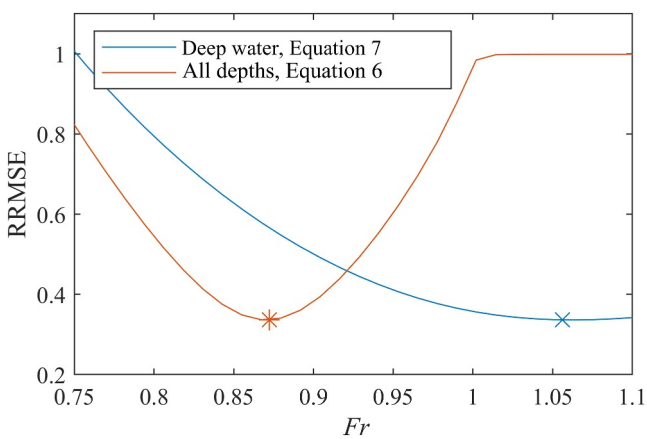

Figure 5. RRMSE for Fr ranging from 0.75 to 1.1.

3.5. Wave Celerity Versus Flow Velocity

We used L and h to estimate wave celerity using both the deep-water and general wave dispersion equations and compared them with the measured U_{ave}, the cross sectionally averaged velocity through the first peak and trough. c_g (Figure 8a) performed better than c_d (Figure 8b), although both overpredicted the velocity. The overprediction of velocity using both equations prompted additional analysis of a more detailed data set of streamwise velocity profiles through the water column at many locations through an UHJ (Hu et al., 2023).

The average surface velocity for three locations across the channel in the first three troughs was 0.94 m/s (9 total measurements of surface velocity in troughs) and 0.77 m/s at the peaks (9 total measurements of surface velocity at peaks). The estimated wave celerity is similar when calculated using the deep-water and general dispersion equations: c_d is 0.90 m/s and c_i is 0.86 m/s. The average (peaks and troughs) measured surface velocity is 0.86 m/s, the same as the estimated c_g. The average velocities at the water surface of the Hu

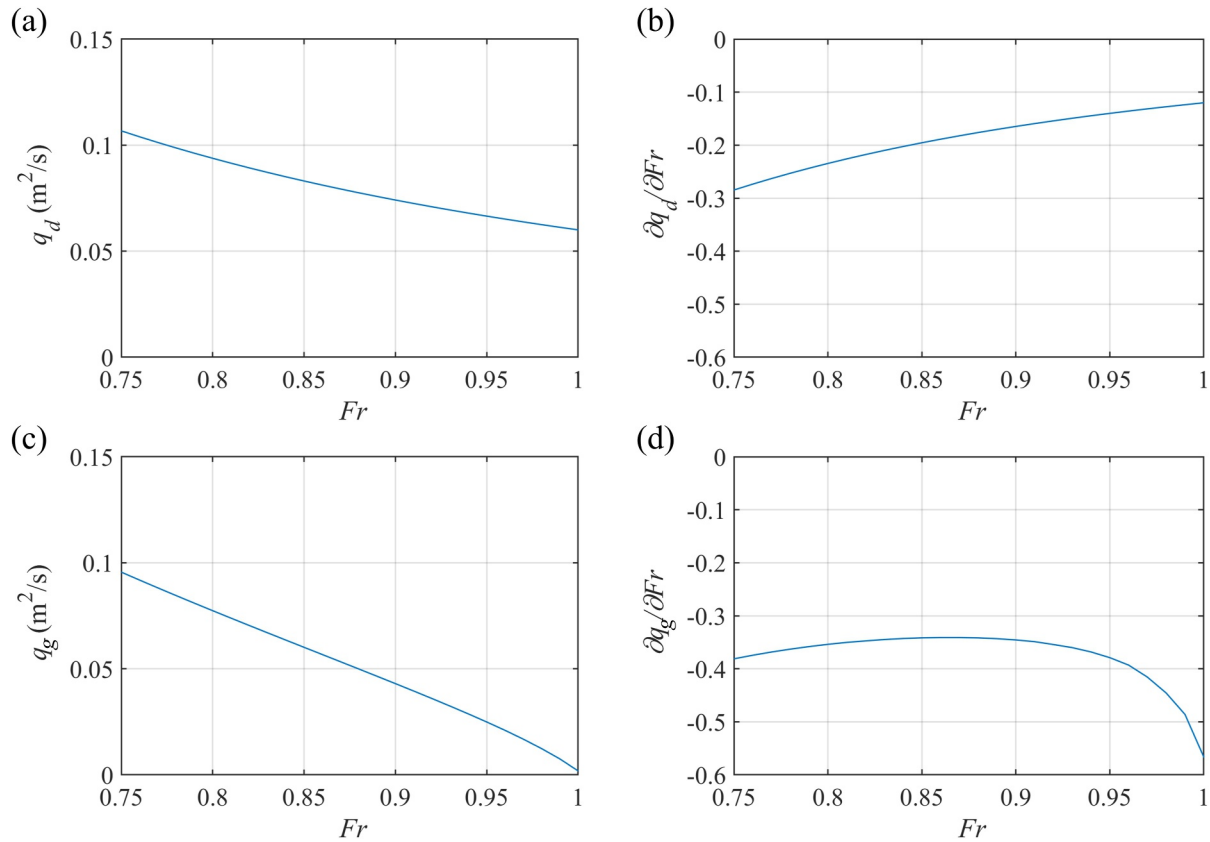

Figure 6. Sensitivity analysis of deep-water and general discharge estimation to Fr. Panel (a) estimated discharge, q_d with varied Fr. Panel (b) change of q_d with Fr over a range of Fr. Panel (c) estimated discharge, q_g with varied Fr (d) change of q_g with Fr over a range of Fr.

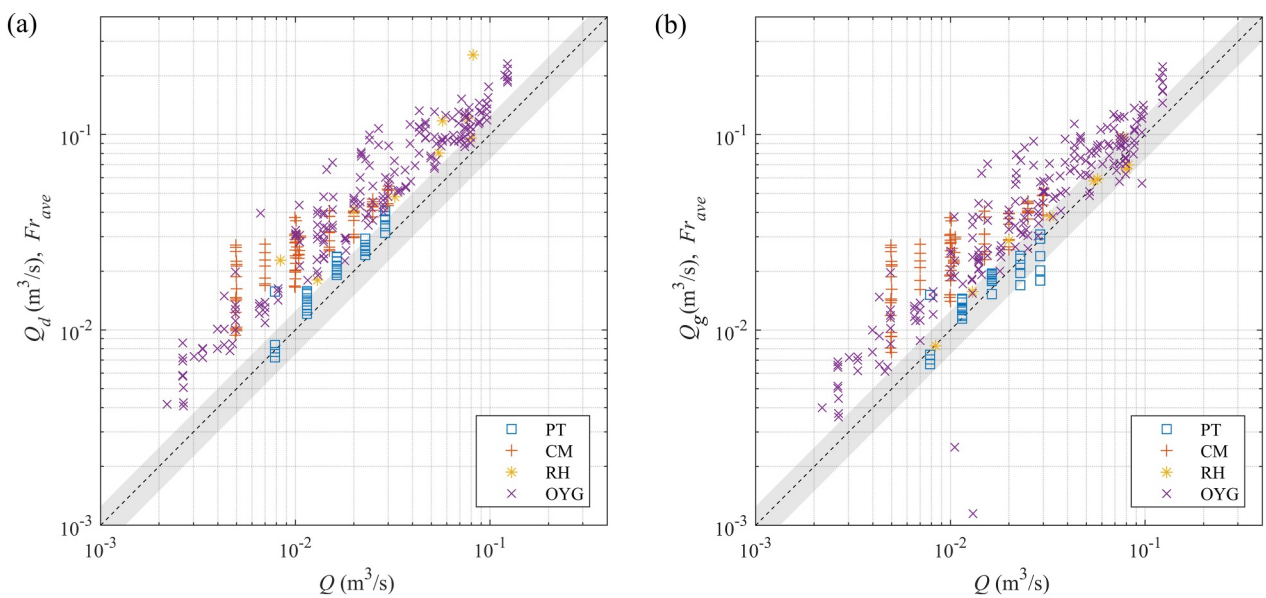

Figure 7. Estimated (y-axis) versus known (x-axis) discharge calculated based on the average Fr of the first peak and trough for each experiment using (a) the deep-water wave dispersion equation and (b) the general wave dispersion equation. The gray band represents 25% error range and the black dashed line is the 1:1 line.

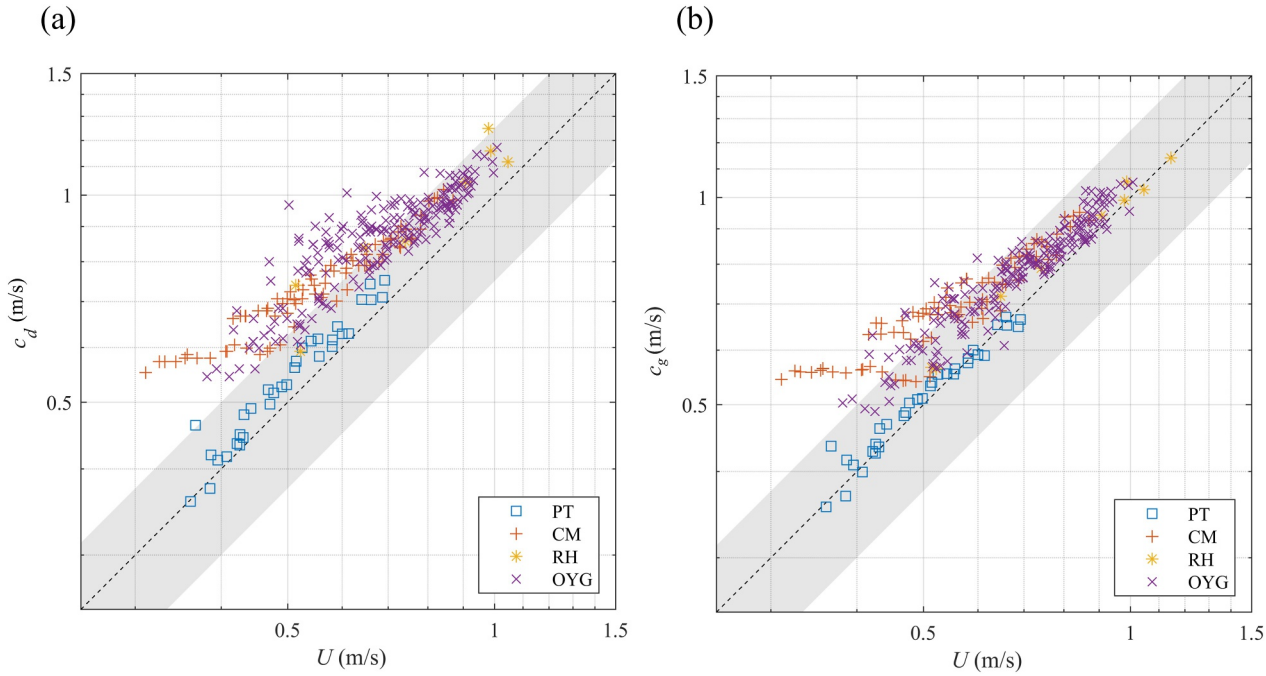

Figure 8. Estimated wave celerity (y-axis) versus cross section averaged velocity through the first peak and trough (x-axis). Panel (a) Celerity computed using the deep-water wave dispersion equation. Panel (b) Celerity computed using the general wave dispersion equation. The gray band represents 25% error range, and the black dashed line is the 1:1 line.

et al. (2023) UHJ experiment were much greater than cross sectionally averaged values, as expected. The cross-sectionally averaged streamwise velocity at the troughs is 0.68 and 0.55 m/s at the peaks, leading to α values (ratio of cross-sectionally averaged velocity to surface velocity) of 0.72 in the troughs and 0.71 at the peaks. For this flume experiment, the estimated wave celerity using both equations was much closer to the measured streamwise surface velocity than the cross-sectionally-averaged velocity. Although this analysis was based on only one flume run, this result highlights the difference between surface and depth-averaged flow velocities in UHJs and that the assumption of $c = U$ is not strictly correct.

The proportionality constant, α, defined here as the ratio of cross-sectionally averaged to surface velocity, was 0.71–0.72 for one experiment. This range is lower than the commonly referenced surface-velocity correction coefficient of approximately 0.85 reported for natural open-channel flows that often exhibit logarithmic velocity profiles (Biggs et al., 2023). To evaluate sensitivity, we conducted a similar analysis to that described in Section 3.3 but also tested the effect of applying the coefficient value of 0.85 that is typically used as a default. We tested this coefficient in both the deep and general wave dispersion equations over a range of possible Fr values to determine the Fr that minimized RRMSE (refer to Figure 9) and compared it with the mean of Fr_{ave} for all experiments combined.

When applying acoefficient of 0.85 to the deep-water equation, RRMSE was minimized at 0.33 by $Fr = 0.83$. Applying the same coefficient to the general dispersion equation, the minimum RRMSE to 0.30 occurred at $Fr = 0.71$. Both results improved upon the RRMSE of the data presented in Figure 4, when using the deep-water equation (Equation 3) assuming $Fr = 1$. The Fr at which both equations were minimized was much closer to Fr_{ave} (0.74, all experiments) than when no coefficient was applied. This pattern suggests that wave celerity in UHJs can approximate surface velocity, but the scaling factor needed to relate surface to depth-averaged velocity is context-dependent and should not be assumed equivalent to uniform-flow correction coefficients.

When applying an α coefficient to the general differential sensitivity analysis, we found that the Fr versus $\partial q_d/\partial Fr$ and of $\partial q_g/\partial Fr$ curves shifted to the left, and that the Fr at which the slope of the curves approached zero decreased. For the general wave dispersion relation, q_g was least sensitive at $Fr = 0.75$, and then increased in sensitivity again as Fr approached 0.84 (refer to Figure 10d). Interestingly, the Fr at which q_g was least sensitive to variation in Fr was very close to the mean of all Fr_{ave} (0.74) when the 0.85 coefficient was applied. At Fr greater than 0.84, $\partial q_g/\partial Fr$

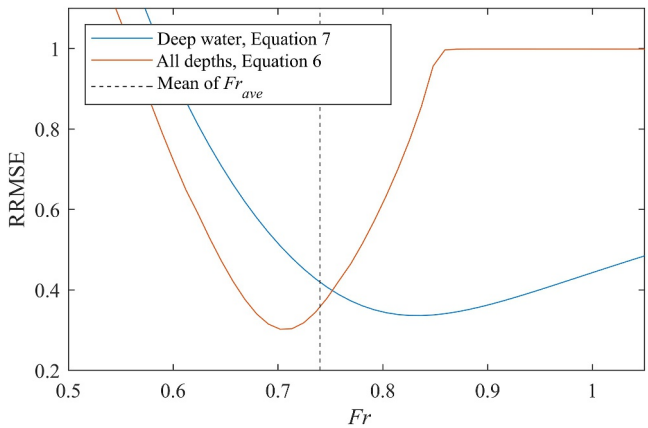

Figure 9. RRMSE resulting from estimates of discharge using $\alpha = 0.85$.

was approximately 0, because at these values, q_g estimates were close to 0. At Fr approaching 1, $\partial q_d/\partial Fr$ approached 0, suggesting that at near critical values, q_d was less sensitive to variation in F. This was also exhibited without an α correction (refer to Figure 6b). The similarity between the Fr at which RRMSE was minimized using the general dispersion equation and measured Fr_{ave} might indicate that applying an α correction factor could lead to a closer approximation of the relationship between celerity and flow velocity. However, because α is context-specific in UHJs, more measurements of width-averaged surface velocity and cross sectionally averaged velocity would help to better constrain its variability and applicability.

We also computed RRMSE of discharge estimates using the measured Fr (Fr_{ave}) for each experiment with a range of α values to investigate the value at which RRMSE was minimized for both wave dispersion equations. In our analysis, the α value at which this occurred was 0.95, quite close to 1. The α value at which the deep-water dispersion equation RRMSE was minimized was 0.84.

4. Discussion

As we describe in Section 1, the goal of this study is to assess assumptions made to estimate discharge in UHJs following the approach outlined by Legleiter et al. (2025) and Dietterich et al. (2022), namely: (a) that Fr is near 1 through standing waves in UHJs, (b) that deep-water conditions are met ($h/L > 0.5$) and (c) that wave celerity is equal to cross-sectionally averaged velocity. We used a compilation of flume data to explore the hydraulic

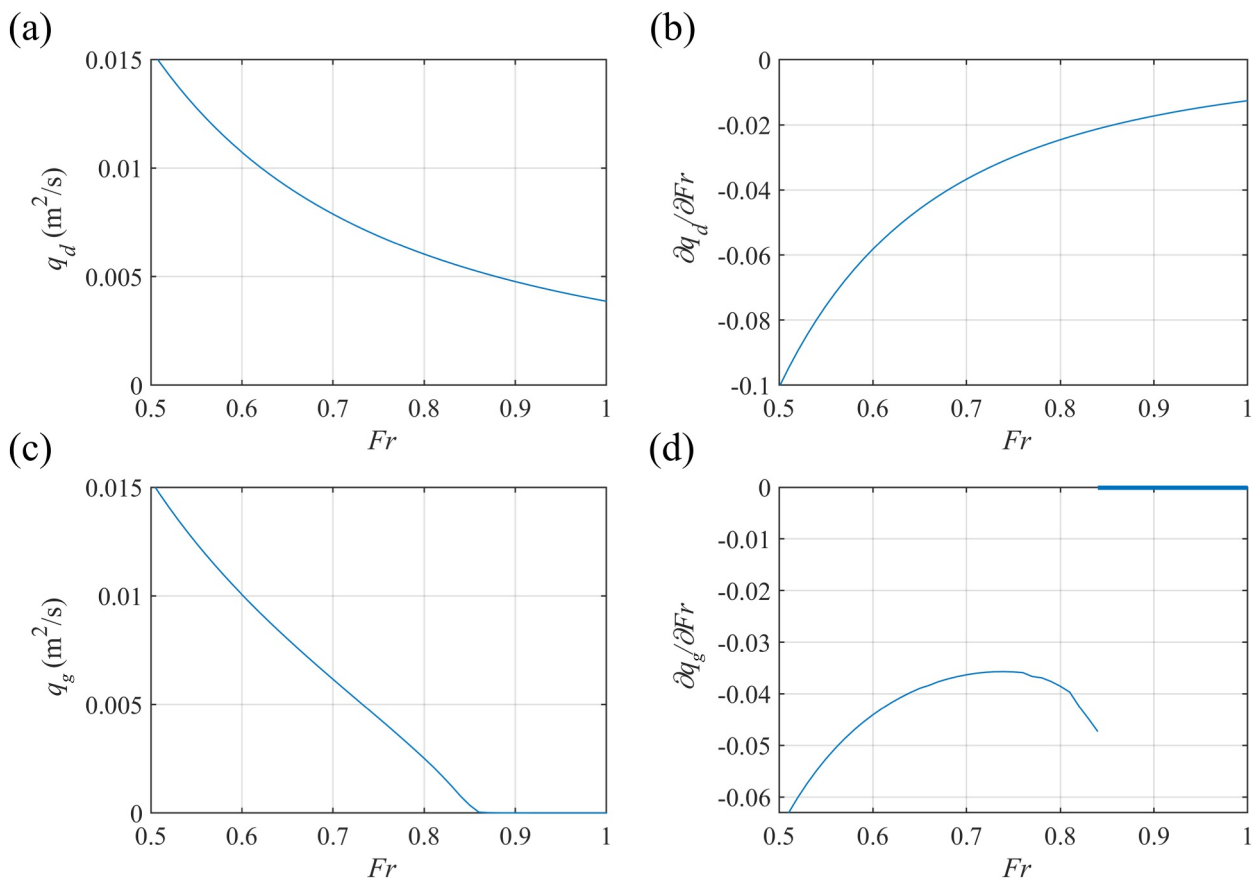

Figure 10. Sensitivity analysis of deep-water and general discharge estimation to Fr when applying an α correction of 0.85. Panel (a) estimated discharge, q_d with varied Fr. Panel (b) change of q_d with Fr over a range of Fr. Panel (c) estimated discharge, q_g with varied Fr (d) Change of q_g with Fr over a range of Fr.

conditions that develop in UHJs and test two wave dispersion relations as a basis for discharge estimation. In this section we discuss the feasibility of applying these methods to estimate discharge in natural channels, the implications of these assumptions, and identify opportunities for further research.

4.1. Discharge Estimate Using Picked *Fr*

Our analysis revealed that although flow conditions approach critical in the troughs of UHJs, Fr_{ave} deviates significantly from 1, which brings into question the assumption of cross-sectionally averaged $Fr = 1$ in UHJs. We do acknowledge, however, the possibility that Fr reported herein was based on measurements of depth at the channel centerline but using the full discharge, and Fr may be closer to 1 at the center of the UHJ. Similarly, we tested the hypothesis that the deep-water assumption is appropriate. Despite the deviation of measured Fr from 1 and the lack of flume data exhibiting deep-water conditions, selecting $Fr = 1$ and using the deep-water wave dispersion equation performed well (RRMSE of 0.35). The discharge estimation results and reported RRMSE values using the deep-water and general wave dispersion equations underscore the sensitivity of these methods to the assumed Fr value.

The general dispersion equation performs better when assuming a subcritical Fr that more closely approximates the value measured in the flume experiments than when selecting a Fr close to 1. When using the deep-water dispersion equation, the influence of flow depth on celerity is ignored. In shallow water, waves are shorter with lower celerity because energy is dissipated through frictional resistance with the bed, even smooth flume bed and walls used in these experiments. By ignoring the influence of shallow depth on wave celerity (and flow velocity by the assumption that $c = U$), velocity is overpredicted using the deep-water equation. By selecting a larger Fr than the measured value (i.e. 1) and solving for depth by using the equation for the definition of the Froude number, depth is underpredicted, which counterbalances the overpredicted velocity. Thus, physically, we would expect that the deep-water equation performs well when given a too large Fr. These findings about discharge estimate sensitivity to Fr and the nature of the wave dispersion equations highlight the potential to improve discharge estimate accuracy by incorporating flexible assumptions (i.e. $Fr = 1$) about flow conditions, particularly when applying these techniques to natural rivers where variability in Fr is inherent.

Well-established texts on open channel hydraulics (Chow, 1959; Henderson, 1966) show using the specific energy equation, $E = h + \frac{U^2}{2g}$, that in rectangular open channels, when wave celerity is equal to and opposite flow velocity, flow is near critical. This holds true only when waves are long, have small amplitude, and there is no significant energy loss through the UHJ (Henderson, 1966). Even for cases when there are no visible surface rollers, energy is dissipated through the formation of a near-bed roller exhibiting velocity reversal below wave crests, through flow separation, and turbulent energy dissipation (Fawer, 1937; Hu et al., 2023; Lauffer, 1935), the historical study of which is described by Hager and Castro-Orgaz (2019). Because flow through the free surface undulations of UHJs is three-dimensional, the assumption that standing waves in UHJs propagate upstream with the same speed as cross-section averaged downstream velocity is difficult to confirm and likely varies over multiple waves. To focus in on the assumption that $c_d = U$ and investigate other potential sources of error, we relaxed the assumption that flow in UHJs is near critical by assessing the performance of the discharge estimates using the measured Fr.

4.2. Wave Celerity Versus Velocity

Discharge estimates using the measured Fr_{ave} for each experiment revealed additional nuances in the performance of the deep-water and general dispersion equations. Both Q_d and Q_g overpredicted discharge, with Q_g demonstrating greater accuracy (RRMSE = 0.53) compared to Q_d (RRMSE = 0.77). Similarly, c_d and c_g overpredicted U. Error in discharge estimates when using Fr_{ave} could be associated with the measurements of depth used to compute velocity and Fr_{ave}, the wavelength measurement used to compute celerity, or error associated with the assumption that wave celerity is equal to cross sectionally averaged velocity. The definition of the Froude number describes the specific energy of cross section-average conditions. However, in UHJs, flow is variable across the channel width, and computing Fr_{ave} using a measurement taken at a single location (often at the channel center) does not fully describe the specific energy state of the entire cross section. Other conditions that may influence the accuracy of measurements used to compute Fr_{ave}, Q_d, and Q_g, include lateral nonuniformity of standing waves (variable wavelength), the presence of lateral shockwaves, and the distribution of flow velocity throughout the cross section.

Although we use only one data point to investigate the assumption that computed wave celerity is equal to the cross sectionally averaged velocity, we found that a more appropriate assumption may be that wave celerity is equal to the surface velocity rather than depth-averaged velocity. The literature describing wave dispersion in rivers is scant. However, studies have shown that the flow field is variable where standing waves form (Kieffer, 1985, 1987; Magirl et al., 2009), which might introduce additional complexity to the wave celerity versus cross-sectionally averaged flow velocity comparison. As described above in Section 4.1, flow separation near the bed has been documented below UHJ wave peaks. If wave celerity more closely approximates surface rather than cross-section-averaged velocity, applying an α coefficient could improve the accuracy of this method. For example, applying an $\alpha = 0.85$ coefficient to correct for $c_d \neq U$ (i.e., $U = 0.85c_d$) and using measured Fr_{ave} of each experiment (not the mean of Fr_{ave}) resulted in an RRMSE of 0.26, the lowest RRMSE that we report in this paper. However, when applying the same coefficient to correct for $c_g \neq U$ and using measured Fr_{ave} the resulting RRMSE was 0.63. It is possible that by applying an α coefficient to the general equation, this over-compensates for the influence of shallow flows on wave dispersion because there is a depth term included in the dispersion equation. Although an α coefficient of 0.85 has widely been documented in rivers (Biggs et al., 2023), additional measurements of the vertical velocity profile in UHJs with a range of inflow and depth conditions may elucidate the relationship between wave celerity and velocity distribution.

In summary, we present three main takeaways.

- Assuming $h/L > 0.5$ (assumption 2) likely leads to overprediction of wave celerity and therefore the assumed cross-section-averaged velocity. However, this error is counterbalanced by assuming that $Fr = 1$ (assumption 1), given that the experimental data indicate that the measured Fr_{ave} is more commonly a subcritical value. We found the mean of Fr_{ave} for the experiments analyzed in this study to be 0.74.
- Assuming that $c = U$ (assumption 3) also leads to overprediction of velocity, even when relaxing assumption 1 by using the measured Fr_{ave} and when eliminating assumption 2 by using the general equation. This error can be accounted for by applying an α coefficient. Additional experimental studies could clarify the relationship between surface and depth-averaged velocities in UHJs to develop an α coefficient best suited to UHJs, which exhibit different velocity profiles than steady uniform open channel flows.
- The deep-water wave dispersion equation is less sensitive to variability of Fr values close to 1. The general equation is highly sensitive to variability of Fr at near-critical values. Thus, when estimating discharge using the general wave dispersion equation, an incorrect assumption of Fr or α can produce large errors. This presents a challenge when measurements are limited to those obtained via remote sensing imagery. Therefore, using the deep-water equation may prove a more practical approach for estimating discharge with observations of channel width and wavelength obtained from remote sensing imagery.

4.3. Relevance in Natural Channels

Each of the data sets that we considered in this study were acquired in rectangular channels with fixed beds. Natural channels exhibit a variety of cross-sectional geometries that have morphodynamic feedbacks commonly associated with channel type (i.e., Montgomery and Buffington (1997)). Channel morphology could influence the presence of UHJs and the proportion of the total channel width they occupy. Uncertainty associated with channel morphology provides an opportunity to further investigate the variability of UHJ characteristics in rivers such as the total width occupied by standing waves, the presence of breaking waves, or the influence of channel slope on discharge estimate accuracy. The bed slope used in many flume experiments in this study was 0%. Grant (1997) and Legleiter et al. (2025) suggest that standing waves most commonly emerge in natural rivers with steep slopes. However, hydraulic jumps, and specifically UHJs, can form at 0% slopes and the development of supercritical inflow conditions and downstream transition to subcritical free surface undulations can be driven by rapid longitudinal changes in hydraulic roughness, channel width, or channel obstructions such as boulders.

Also note that the mean ratio of h_{ave}/L in our flume experiments was approximately 0.2, much less than the deep-water criterion ($h/L > 0.5$). Although h/L ratios in natural rivers are expected to be larger, there is little published data to constrain this relationship, and further study could provide additional insights. Additionally, in the flume experiments wavelength was of the same order as channel width ($L \sim B$), whereas in natural rivers wavelength is typically much smaller than width ($L \ll B$) (e.g., Kieffer, 1987; Grant, 1997; Magirl et al., 2009). This contrast

provides an opportunity to investigate how channel width influences UHJ wavelength and celerity in natural settings.

4.3.1. Estimating Discharge Using Remote Sensing Imagery

Legleiter et al. (2025) describe an approach to estimating discharge from readily available image data that only requires measurements of channel width and wavelength. Their framework implicitly assumes that the standing wave trains identified in imagery correspond to undular hydraulic jumps as defined in hydraulic literature. Our flume data analysis does not independently verify that interpretation in natural rivers but instead evaluates the hydraulic implications of that assumption under controlled UHJ conditions. This simple method could become a useful tool in the typical situation where site-specific information on Fr and/or α is not available. Although our analysis indicates that the assumptions made by Legleiter et al. (2025) are not strictly satisfied, the accuracy of the method could be improved by utilizing additional data such as measurements of Fr and α to correct for the $c = U$ assumption. Despite these limitations, initial testing suggests that the method is robust and can provide reasonably accurate estimates of discharge based on Equation 3. However, the critical flow approach could be further enhanced by making measurements in UHJs to inform estimates of Fr or α that are based on wave and channel characteristics that could be identified in remote sensing imagery.

Another practical implication of our results is the need to carefully consider whether standing waves observed in remote sensing imagery can be confidently interpreted as UHJs or surface manifestations of near-critical flow conditions. Current remote sensing applications (e.g., Dietterich et al., 2022; Legleiter et al., 2025) assume that periodic free-surface undulations downstream of a hydraulic control indicate Fr ≈ 1 and c ≈ U, but do not offer an objective diagnostic to verify that those waves correspond to an UHJ. Our experimental findings show that even in controlled UHJs, wave celerity and flow velocity diverge and Fr departs from unity, implying that real-world systems with spatially variable turbulence, channel form, and interactions between flow and sediment might also deviate further from these assumptions. While modern imagery allows reliable identification of surface waves, how to distinguish UHJs from other wave types (e.g., roughness-induced standing waves, reflected waves, or dispersive oscillations unrelated to critical flow) remains an open question.

Therefore, although visual identification of standing waves provides a convenient starting point for preliminary reconnaissance, operational discharge estimation using this approach will require development of robust classification criteria, potentially combining spectral analysis, multi-angle or UAV imagery, and targeted hydrodynamic measurements, to gain confidence that standing-wave fields represent near-critical flow conditions.

5. Conclusion

In this study, we investigate the feasibility of estimating discharge via the method described by Dietterich et al. (2022) and Legleiter et al. (2025) by testing key assumptions using experimental flume data sets. These assumptions include near-critical flow conditions, the applicability of a deep-water approximation, and the equality of wave celerity and cross-sectionally averaged flow velocity in undular hydraulic jumps. Our results indicate that the conditions required by these assumptions are often unmet in the flume experiments and that discharge estimates are sensitive to changes in Fr. However, estimated discharges scatter around the 1:1 line relative to measured values, suggesting that departures from idealized assumptions do not necessarily preclude reasonable agreement under laboratory confirmed UHJ conditions. We show that the estimated wave celerity more closely approximates surface velocity than cross-sectional-averaged velocity in one experimental flume run. For the situation where α (the ratio of depth-averaged-to-surface velocity) is assumed to be 0.85, estimate for Q_d using Fr_{ave} of each experiment, produce an RRMSE of 0.25. Thus, when relaxing the assumption that $Fr = 1$ and applying an α coefficient to correct for the overestimate of velocity due to the deep-water assumption, the most accurate discharge estimate is made. Because application of this framework to remotely sensed imagery assumes that the observed wave trains correspond to undular hydraulic jumps, the utility of the method in natural rivers ultimately may depend on the accuracy of that interpretation. Further testing this method in flumes and natural rivers and measuring hydraulic conditions and standing wave characteristics could yield additional insight on factors that might influence discharge estimate accuracy. Additionally, future research could investigate the relationship between wave celerity and depth-averaged velocity in UHJs to refine this discharge estimation method.

Notation

α	Ratio of surface flow velocity to cross-section-averaged flow velocity
B	Channel width (m)
c	Wave celerity (m/s)
c_g	Wave celerity for general water depth (m/s)
c_d	Wave celerity for deep water depth (m/s)
Fr	Froude number $\frac{U}{\sqrt{gh}}$
Fr_1	Inflow Froude number
Fr_t	Froude number computed in the first trough
Fr_p	Froude number computed at the first peak
Fr_{ave}	Average of Fr_t and Fr_p
g	Acceleration due to gravity, (9.81 m^2/s)
h	Flow depth (m)
h_1	Inflow depth (m)
h_c	Critical depth (m)
h_p	Flow depth at first wave peak (m)
h_t	Flow depth at first wave trough (m)
h_{ave}	Average of h_p and h_t
L	Undular hydraulic jump wavelength (m)
Q	Discharge (m^3/s)
Q_d	Estimated discharge using deep water wave dispersion equation (m^3/s)
Q_g	Estimated discharge using general wave dispersion equation (m^3/s)
q	Discharge per unit width (m^2/s)
Re_1	Inflow Reynolds number
U	Cross-sectionally averaged velocity (m/s)
S	Channel slope (m/m)

Conflict of Interest

The authors declare no conflicts of interest relevant to this study.

Data Availability Statement

The data used in this study were kindly shared by the authors of the original flume studies that are cited throughout the manuscript (Chanson & Montes, 1995; Gotoh et al., 2004; Hu et al., 2023; Ohtsu et al., 2001, 2003; Pasha & Tanaka, 2017; Reinauer & Hager, 1995).

Acknowledgments
Funding for this project is provided through the USGS Next Generation Water Observing System (NGWOS).

References

Airy, G. B. (1845). On tides and waves. *Encyclopedia Metropolitana*, *5*, 241–396.
Andreadis, K. M., Coss, S. P., Durand, M., Gleason, C. J., Simmons, T. T., Tebaldi, N., et al. (2025). A first look at river discharge estimation from SWOT satellite observations. *Geophysical Research Letters*, *52*(9), e2024GL114185. https://doi.org/10.1029/2024GL114185

Biggs, H., Smart, G., Doyle, M., Eickelberg, N., Aberle, J., Randall, M., & Detert, M. (2023). Surface velocity to depth-averaged Velocity—A review of methods to estimate alpha and remaining challenges. *Water*, *15*(21), 3711. https://doi.org/10.3390/w15213711

Bjerklie, D. M., Moller, D., Smith, L. C., & Dingman, S. L. (2005). Estimating discharge in rivers using remotely sensed hydraulic information. *Journal of Hydrology*, *309*(1), 191–209. https://doi.org/10.1016/j.jhydrol.2004.11.022

Castro-Orgaz, O., & Chanson, H. (2022). Free surface profiles of near-critical instabilities in open channel flows: Undular hydraulic jumps. *Environmental Fluid Mechanics*, *22*(2), 275–300. https://doi.org/10.1007/s10652-021-09797-3

Castro-Orgaz, O., & Hager, W. H., & Springer International Publishing AG. (2017). *Non-hydrostatic free surface flows*. Springer.

Castro-Orgaz, O., Hager, W. H., & Dey, S. (2015). Depth-averaged model for undular hydraulic jump. *Journal of Hydraulic Research*, *53*(3), 351–363. https://doi.org/10.1080/00221686.2014.967820

Chanson, H. (1993). *Characteristics of undular hydraulic jumps. Research report no. CE146, department of civil engineering*. The University of Queensland.

Chanson, H. (2004). *Hydraulics of open channel flow*. Elsevier.

Chanson, H. (2009). Current knowledge in hydraulic jumps and related phenomena. A survey of experimental results. *European Journal of Mechanics—B: Fluids*, *28*(2), 191–210. https://doi.org/10.1016/j.euromechflu.2008.06.004

Chanson, H., & Montes, J. S. (1995). Characteristics of undular hydraulic jumps: Experimental apparatus and flow patterns. *Journal of Hydraulic Engineering*, *121*(2), 129–144. https://doi.org/10.1061/(ASCE)0733-9429(1995)121:2(129)

Chow, V. T. (1959). *Open-channel hydraulics*. McGraw-Hill Civil Engineering Series.

Dietterich, H. R., Grant, G. E., Fasth, B., Major, J. J., & Cashman, K. V. (2022). Can lava flow like water? Assessing applications of critical flow theory to channelized basaltic lava flows. *Journal of Geophysical Research: Earth Surface*, *127*(9), e2022JF006666. https://doi.org/10.1029/2022JF006666

Durand, M., Gleason, C., Garambois, P.-A., Bjerklie, D., Smith, L., Roux, H., et al. (2016). An intercomparison of remote sensing river discharge estimation algorithms from measurements of river height, width, and slope. *Water Resources Research*, *52*(6), 4527–4549. https://doi.org/10.1002/2015wr018434

Durand, M., Gleason, C. J., Pavelsky, T. M., Prata de Moraes Frasson, R., Turmon, M., David, C. H., et al. (2023). A framework for estimating global river discharge from the surface water and ocean topography satellite mission. *Water Resources Research*, *59*(4), e2021WR031614. https://doi.org/10.1029/2021WR031614

Fawer, C. (1937). Etude de quelques écoulements permanents à filets courbes.

Gotoh, H., Yasuda, Y., & Ohtsu, I. (2004). Effect of channel slope on flow characteristics of undular hydraulic jumps. *Journal of Applied Mechanics*, *7*, 953–960. https://doi.org/10.2208/journalam.7.953

Grant, G. E. (1997). Critical flow constrains flow hydraulics in mobile-bed streams: A new hypothesis. *Water Resources Research*, *33*(2), 349–358. https://doi.org/10.1029/96wr03134

Grillhofer, W., & Schneider, W. (2003). The undular hydraulic jump in turbulent open channel flow at large Reynolds numbers. *Physics of Fluids*, *15*(3), 730–735. https://doi.org/10.1063/1.1538249

Hager, W. H., & Castro-Orgaz, O. (2019). ON the undular hydraulic jump and the undular surge. In *Presented at the 38th IAHR World Congress* (pp. 2030–2039). https://doi.org/10.3850/38WC092019-0414

Henderson, F. M. (1966). *Open channel flow* (Vol. 522). Macmillan.

Hu, H., Wang, H., Pan, D., Wang, X., & Bai, R. (2023). Free-surface undulation and velocity turbulence in shallow undular hydraulic jumps. *Ocean Engineering*, *269*, 113566. https://doi.org/10.1016/j.oceaneng.2022.113566

Jodeau, M., Hauet, A., Paquier, A., Le Coz, J., & Dramais, G. (2008). Application and evaluation of LS-PIV technique for the monitoring of river surface velocities in high flow conditions. *Flow Measurement and Instrumentation*, *19*(2), 117–127. https://doi.org/10.1016/j.flowmeasinst.2007.11.004

Jurisits, R., & Schneider, W. (2012). Undular hydraulic jumps arising in non-developed turbulent flows. *Acta Mechanica*, *223*(8), 1723–1738. https://doi.org/10.1007/s00707-012-0666-4

Kasvi, E., Salmela, J., Lotsari, E., Kumpula, T., & Lane, S. (2019). Comparison of remote sensing based approaches for mapping bathymetry of shallow, clear water rivers. *Geomorphology*, *333*, 180–197. https://doi.org/10.1016/j.geomorph.2019.02.017

Kennedy, J. F. (1961). *Stationary waves and antidunes in alluvial channels*. California Institute of Technology.

Kennedy, J. F. (1963). The mechanics of dunes and antidunes in erodible-bed channels. *Journal of Fluid Mechanics*, *16*(4), 521–544. https://doi.org/10.1017/s0022112063000975

Keulegan, G. H. (1938). *Laws of turbulent flow in open channels*. National Bureau of Standards.

Kieffer, S. W. (1985). The 1983 hydraulic jump in crystal rapid: Implications for river-running and geomorphic evolution in the grand canyon. *The Journal of Geology*, *93*(4), 385–406. https://doi.org/10.1086/628962

Kieffer, S. W. (1987). The rapids and waves of the Colorado River, Grand Canyon, Arizona. *U.S. Geological Survey Open File Report*, *87*(96), 69.

Lamb, H. (1924). *Hydrodynamics*. University Press.

Lauffer, H. (1935). Wassersprung bei kleinen Sprunghöhen. *Wasserwirtschaft Und Technik*, *28*(11/12), 137–140.

Le Coz, J., Jodeau, M., Hauet, A., Marchand, B., & Le Boursicaud, R. (2014). Image-based velocity and discharge measurements in field and laboratory river engineering studies using the free FUDAA-LSPIV software. In *Presented at the Proceedings of the International Conference on fluvial hydraulics, River flow* (Vol. 3, p. 7).

Legleiter, C. J. (2021). The optical river bathymetry toolkit. *River Research and Applications*, *37*(4), 555–568. https://doi.org/10.1002/rra.3773

Legleiter, C. J., Grant, G., Bae, I., Fasth, B., Yager, E., White, D. C., et al. (2025). Remote sensing of river discharge based on critical flow theory. *Geophysical Research Letters*, *52*(9), e2025GL114851. https://doi.org/10.1029/2025GL114851

Legleiter, C. J., & Kinzel, P. J., III. (2021). Surface flow velocities from space: Particle image velocimetry of satellite video of a large, sediment-laden river. *Frontiers in Water*, *3*, 652213. https://doi.org/10.3389/frwa.2021.652213

Legleiter, C. J., Roberts, D. A., & Lawrence, R. L. (2009). Spectrally based remote sensing of river bathymetry. *Earth Surface Processes and Landforms*, *34*(8), 1039–1059. https://doi.org/10.1002/esp.1787

Magirl, C. S., Gartner, J. W., Smart, G. M., & Webb, R. H. (2009). Water velocity and the nature of critical flow in large rapids on the Colorado River, Utah. *Water Resources Research*, *45*(5). https://doi.org/10.1029/2009WR007731

Montes, J., & Chanson, H. (1998). Characteristics of undular hydraulic jumps: Experiments and analysis. *Journal of Hydraulic Engineering*, *124*(2), 192–205. https://doi.org/10.1061/(asce)0733-9429(1998)124:2(192)

Montgomery, D. R., & Buffington, J. M. (1997). Channel-reach morphology in mountain drainage basins. *Geological Society of America Bulletin*, *109*(5), 596–611. https://doi.org/10.1130/0016-7606(1997)109<0596:crmimd>2.3.co;2

Ohtsu, I., Yasuda, Y., & Gotoh, H. (2001). Hydraulic condition for undular-jump formations. *Journal of Hydraulic Research*, *39*(2), 203–209. https://doi.org/10.1080/00221680109499821

Ohtsu, I., Yasuda, Y., & Gotoh, H. (2003). Flow conditions of undular hydraulic jumps in horizontal rectangular channels. *Journal of Hydraulic Engineering*, *129*(12), 948–955. https://doi.org/10.1061/(ASCE)0733-9429(2003)129:12(948)

Pasha, G. A., & Tanaka, N. (2017). Undular hydraulic jump formation and energy loss in a flow through emergent vegetation of varying thickness and density. *Ocean Engineering*, *141*, 308–325. https://doi.org/10.1016/j.oceaneng.2017.06.049

Pasha, G. A., & Tanaka, N. (2019). Critical resistance affecting sub-to super-critical transition flow by vegetation. *Journal of Earthquake and Tsunami*, *13*(1), 1950004. https://doi.org/10.1142/s1793431119500040

Phillips, O. M. (1977). The dynamics of the upper ocean. *(No Title)*.

Pond, S. (1983). *Introductory dynamical oceanography*. Pergamon Press Ltd.

Recking, A., Bacchi, V., Naaim, M., & Frey, P. (2009). Antidunes on steep slopes. *Journal of Geophysical Research*, *114*(F4). https://doi.org/10.1029/2008JF001216

Reinauer, R., & Hager, W. H. (1995). Non-breaking undular hydraulic jump. *Journal of Hydraulic Research*, *33*(5), 683–698. https://doi.org/10.1080/00221689509498564

Roy Biswas, T., Dey, S., & Sen, D. (2021). Undular hydraulic jumps: Critical analysis of 2D RANS-VOF simulations. *Journal of Hydraulic Engineering*, *147*(11), 06021017. https://doi.org/10.1061/(ASCE)HY.1943-7900.0001939

Schweitzer, S. A., & Cowen, E. A. (2021). Instantaneous river-wide water surface velocity field measurements at centimeter scales using infrared quantitative image velocimetry. *Water Resources Research*, *57*(8), e2020WR029279. https://doi.org/10.1029/2020wr029279

Stokes, G. G. (1847). On the theory of oscillatory waves. *Transactions of the Cambridge Philosophical Society*, *8*, 441–455.

Sturm, T. W. (2001). *Open channel hydraulics* (Vol. 1). McGraw-Hill.